

# Antiviral Activity of Nanostructured Brazilian Green Propolis Against Herpes Simplex Virus Type 2: Mechanistic Insights and Translational Potential for Reproductive Health

Shulin Li<sup>1</sup>, Muhammad Usman Elahi Siddiqui<sup>2</sup>, Sreemoy Kanti Das<sup>3\*</sup>

<sup>1</sup> Ph.D. Candidate, MD, Faculty of Medicine, Lincoln University College, Malaysia

<sup>2</sup> Khan Sahab Dr Rahmat Elahi Memorial Welfare Trust, Pakistan

<sup>3\*</sup> Professor, Faculty of Pharmacy, Lincoln University College, Malaysia (Corresponding Author)

Email: [sreemoy@lincoln.edu.my](mailto:sreemoy@lincoln.edu.my)

## ABSTRACT

### Background

Herpes simplex virus type 2 (HSV-2) infects more than 500 million people worldwide and remains a major cause of recurrent genital infections. Brazilian green propolis has demonstrated antiviral activity against herpesviruses; however, its clinical application is limited by poor aqueous solubility and low bioavailability.

### Objectives

This study aimed to develop a nanostructured formulation of Brazilian green propolis and evaluate its antiviral activity against HSV-2 while investigating the underlying mechanism of action.

### Methods

Brazilian green propolis extract was incorporated into a microemulsion-based nanostructured system. Particle size was characterized using dynamic light scattering (DLS) and transmission electron microscopy (TEM). Cytotoxicity was assessed using the MTT assay in Vero cells. Antiviral activity was evaluated using plaque reduction assays and time-of-addition experiments. Viral replication kinetics were analyzed using TCID<sub>50</sub> assays.

### Results

The nanostructured formulation produced uniform spherical particles with a mean diameter of 187 nm (PDI = 0.21). Both non-nanostructured and nanostructured propolis exhibited comparable cytotoxicity (CC<sub>50</sub>: 0.024% vs. 0.026%, \*p\* > 0.05) and antiviral potency (IC<sub>50</sub>: 0.003% vs. 0.004%, \*p\* > 0.05). The nanostructured formulation achieved a 44% higher selectivity index (86.7 vs. 60.0). Time-of-addition assays demonstrated that propolis primarily exerts direct virucidal activity, with >98% inhibition upon virus pre-treatment but only 23–26% inhibition post-adsorption. Despite minimal intracellular activity, nanostructured propolis suppressed viral replication over 96 h, with a 2.78 log<sub>10</sub> reduction at 72 h.

### Conclusion

Nanostructured Brazilian green propolis retains full antiviral potency against HSV-2 while significantly improving the selectivity index. The primary mechanism is direct virucidal action, with sustained suppression via an "extracellular trap" mechanism. These findings support further development of propolis-based topical antiviral strategies for reproductive health applications.

**Keywords:** Brazilian green propolis; nanostructured formulation; herpes simplex virus type 2; virucidal mechanism; assisted reproductive technology; selectivity index; artemisinin C; microemulsion

**How to cite this article:** Li S, Siddiqui MUE, Das SK. Antiviral Activity of Nanostructured Brazilian Green Propolis Against Herpes Simplex Virus Type 2: Mechanistic Insights and Translational Potential for Reproductive Health. *Int J Drug Deliv Technol.* 2026;16(22s): 598-604. DOI: 10.25258/ijddt.16.22s.72

**Source of support:** Nil.

**Conflict of interest:** None

## 1. Introduction

Herpes simplex virus type 2 (HSV-2) infects an estimated 520 million people worldwide (13.3% of the global population) and causes approximately 25 million new infections annually.<sup>1</sup> Following primary infection, HSV-2 establishes lifelong latency in sacral dorsal root ganglia, with periodic reactivation leading

to symptomatic genital lesions or asymptomatic viral shedding that sustains transmission.<sup>2</sup> Beyond direct morbidity, HSV-2 infection triples the risk of HIV acquisition,<sup>3</sup> contributing an estimated 420,000 HIV infections annually.<sup>4</sup>

Current management relies on nucleoside analogues (acyclovir, valacyclovir, famciclovir) which inhibit

viral DNA polymerase. Although effective, these agents do not eradicate latent virus, and long-term use is associated with emerging resistance, particularly in immunocompromised populations.<sup>5</sup>

The therapeutic dilemma is especially acute for individuals undergoing assisted reproductive technologies (ART), including in vitro fertilization (IVF). Genital herpes recurrence can disrupt embryo transfer cycles, leading to cancellation and psychological distress.<sup>6</sup> Although acyclovir is generally considered safe during pregnancy, periconceptional use raises patient and clinician concerns.<sup>7</sup>

Propolis, a resinous hive product collected by honeybees, has been used medicinally for centuries owing to its broad-spectrum antimicrobial and anti-inflammatory properties.<sup>8</sup> Brazilian green propolis, derived predominantly from *Baccharis dracunculifolia*, is distinguished by high concentrations of prenylated phenylpropanoids—particularly artepillin C—along with flavonoids and phenolic acids.<sup>9</sup> Its anti-herpesvirus activity has been documented since the 1990s, with multiple studies confirming efficacy against HSV-1 and HSV-2 in vitro.<sup>10–12</sup>

However, clinical application of crude propolis extracts is limited by poor aqueous solubility, low oral bioavailability, and instability under physiological conditions.<sup>13</sup> Nanostructured drug delivery systems offer a rational approach to overcome these limitations. Lipid-based nanocarriers, including microemulsions and nanoemulsions, can enhance solubility, protect bioactive compounds, and improve cellular uptake.<sup>14</sup> Recent studies show that nanoparticle-encapsulated propolis exhibits enhanced anti-HSV-2 activity.<sup>15</sup>

Therefore, this study aimed to develop a nanostructured topical formulation of Brazilian green propolis and elucidate its mechanism of action against HSV-2. The specific objectives were: (1) to prepare and characterize nanostructured propolis; (2) to determine cytotoxicity profiles; (3) to establish dose-response curves and  $IC_{50}$  values; (4) to elucidate the antiviral mechanism; (5) to assess viral replication kinetics; and (6) to interpret findings within the context of reproductive health.

## 2. Materials and Methods

### 2.1 Propolis Extract and Reagents

Brazilian green propolis raw material (Minas Gerais, Brazil) was processed by maceration in 70% ethanol (1:10 w/v) for 7 days at room temperature, filtered to obtain a stock solution. This stock was used for both

non-nanostructured and nanostructured formulations. Acyclovir (GlaxoSmithKline, UK) was prepared as 1 mg/mL stock. MTT reagent was from KeyGEN BioTECH (Nanjing, China). Cell culture media and supplements were from Gibco (Thermo Fisher Scientific, USA).

### 2.2 Cells and Virus

Vero cells (ATCC CCL-81) were maintained in DMEM with 10% fetal bovine serum, 2 mM L-glutamine, 100 U/mL penicillin, 100  $\mu$ g/mL streptomycin, and 0.25  $\mu$ g/mL amphotericin B at 37°C in 5% CO<sub>2</sub>. The HSV-2 wild-type strain was isolated from a patient with primary genital herpes; identity was confirmed by real-time PCR using HSV-2 specific primers (US4 region). Virus stocks were propagated in Vero cells, titrated by plaque assay, and stored at –80°C.<sup>16</sup>

### 2.3 Preparation of Nanostructured Propolis

Nanostructured propolis was prepared using a microemulsion technique adapted from established protocols.<sup>17,18</sup> The optimized formulation consisted of: oil phase – medium-chain triglycerides (6% w/w), Span 80 (4% w/w); aqueous phase – Tween 80 (10% w/w), deionized water (76% w/w); propolis extract (4% w/w) dissolved in ethanol (final ethanol <2%). The aqueous phase was added dropwise to the oil phase under magnetic stirring, followed by high-shear homogenization (13,000 rpm, 5 min) and rotary evaporation to remove ethanol. Non-nanostructured propolis control was prepared by dissolving propolis dry extract in ethanol and diluting directly in cell culture medium (final ethanol  $\leq$ 0.1%). The preparation process is illustrated in Figure 1.



Figure 1. Schematic representation of the microemulsion preparation process for nanostructured Brazilian green propolis

**Figure 1.** Schematic of microemulsion preparation for nanostructured propolis. MCT (6%) and Span 80 (4%) as oil phase; Tween 80 (10%) and water (76%) as aqueous phase; 4% propolis extract. Homogenization yields spherical nanoparticles (mean 187 nm).

### 2.4 Physicochemical Characterization

#### 2.4.1 Particle Size Analysis by Dynamic Light Scattering

Particle size distribution and polydispersity index (PDI) were determined by dynamic light scattering (TopSizer, Omec Instruments, China) at 25°C (detection angle 90°).<sup>19</sup>

#### 2.4.2 Morphological Assessment by Transmission Electron Microscopy

Morphological examination was performed by transmission electron microscopy (JEM-1400Flash, JEOL, Japan) at 80 kV. The nanostructured formulation was diluted, deposited on formvar-coated copper grids, negatively stained with 2% uranyl acetate, and air-dried.<sup>20</sup> Particle diameter was measured from TEM images using ImageJ (NIH, USA).

## 2.5 Cytotoxicity Assay

Cytotoxicity was assessed by MTT assay.<sup>21</sup> Vero cells were seeded in 96-well plates ( $2 \times 10^4$  cells/well) for 24 h. Serial two-fold dilutions of propolis formulations (0.05% to 0.00078%) were added in replicates. After 72 h, MTT (5 mg/mL) was added for 4 h, formazan crystals solubilized in DMSO, and absorbance measured at 490 nm. Cell viability was calculated relative to untreated controls.  $CC_{50}$  was calculated by the Reed-Muench method and confirmed by four-parameter logistic curve fitting (drc package in R).<sup>22</sup> Maximum non-cytotoxic concentration (MNCC) was defined as the highest concentration maintaining  $\geq 90\%$  viability. Morphological changes are shown in Figure 2.

Figure 2. Morphological observation of Vero cells in cytotoxicity assay

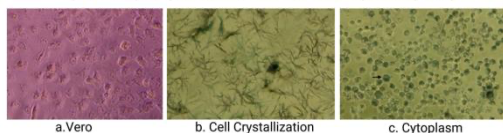


**Figure 2.** Vero cell morphology. (a) Normal monolayer; (b) formazan crystals in viable cells; (c) cytotoxic changes at high propolis concentration.

## 2.6 Antiviral Activity Assays

### 2.6.1 Determination of $IC_{50}$

HSV-2 ( $2 \times 10^3$  PFU/well) was incubated with equal volumes of serial two-fold dilutions of propolis formulations (starting from MNCC) for 1 h at room temperature.<sup>23</sup> Virus-propolis mixtures were added to Vero cell monolayers (6 replicates per concentration) for 1 h at 37°C. After washing, maintenance medium was added and plates incubated until  $>90\%$  CPE in virus controls (72–96 h). Inhibition (%) was calculated from MTT absorbance.  $IC_{50}$  was calculated by the Reed-Muench method and confirmed by nonlinear regression. Representative dose-response curves are presented in Figure 3.

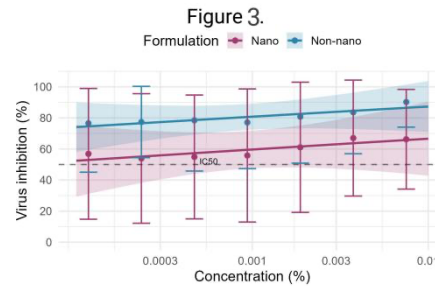


**Figure 3.** Dose-response curves for HSV-2 inhibition by non-nano (purple) and nano (blue) propolis.  $IC_{50}$  = 0.003% (non-nano) and 0.004% (nano). Data are mean  $\pm$  SD (n=18).

### 2.6.2 Time-of-Addition Assay

Four experimental conditions were evaluated at MNCC with 14 replicates per condition per experiment.<sup>24</sup>

**Virus pre-treatment:** HSV-2 incubated with propolis (1 h, RT), then added to cells.

**Cell pre-treatment:** Cells incubated with propolis (2 h, 37°C), washed, then infected.

**Adsorption period:** Propolis present only during virus adsorption (1 h).

**Post-adsorption:** Propolis added after virus adsorption and maintained.

After 72 h under methylcellulose overlay, plaques were counted. Suppression (%) =  $[1 - (\text{mean plaques treated} / \text{mean plaques virus control})] \times 100$ . Acyclovir (20  $\mu\text{g/mL}$ ) was used as positive control. Results are presented in Figure 4.

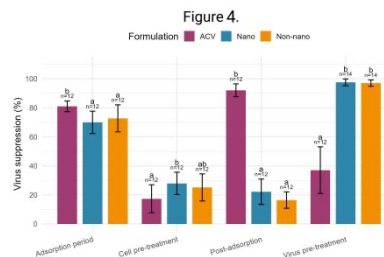


**Figure 4.** Mechanism of antiviral action. Virus pre-treatment achieved  $>98\%$  plaque reduction. ACV, acyclovir.

### 2.6.3 Viral Replication Kinetics

Vero cell monolayers were infected with HSV-2 at MOI 0.1 for 1 h, washed, and incubated with maintenance medium containing nanostructured propolis at MNCC (or medium only for controls). Supernatants were collected at 24, 48, 72, and 96 h and stored at  $-80^\circ\text{C}$ . Viral titers were determined by  $TCID_{50}$  endpoint dilution in Vero cells and calculated by the Reed-Muench method. Replication kinetics are shown in Figure 14, and morphological changes during the assay are shown in Figure 5.

# Antiviral Activity of Nanostructured Brazilian Green Propolis Against Herpes Simplex Virus Type 2: Mechanistic Insights and Translational Potential for Reproductive Health

Figure 5. Morphological changes of Vero cells during viral replication kinetics assay



**Figure 5.** Vero cell morphology at 48 h. (a) Untreated control with CPE; (b) Nano-propolis-treated culture with intact monolayer.

## 2.7 Statistical Analysis

Sample size was calculated based on pilot experiments using G\*Power software. Data were expressed as mean  $\pm$  SD. Normality was assessed by Shapiro-Wilk test and homogeneity of variances by Levene's test. For comparisons between two groups, Student's t-test was used. For multiple group comparisons, one-way ANOVA followed by Tukey's post-hoc test was performed. Two-way ANOVA (time  $\times$  treatment) was used for replication kinetics data. A  $*p^*$ -value  $< 0.05$  was considered statistically significant.

## 3. Results

### 3.1 Physicochemical Characterization

#### 3.1.1 Particle Size Distribution

Non-nanostructured propolis exhibited a broad, polydisperse distribution ( $D_{50} = 1.797 \mu\text{m}$ ). Nanostructured propolis showed a narrow, monomodal distribution with  $D_{50} = 187 \text{ nm}$ ,  $PDI = 0.21$ . Specific surface area increased 8.9-fold to  $32.828 \text{ m}^2/\text{g}$  (Table 1, Figure 6).

Table 1. Particle size distribution parameters of propolis formulations

Parameter	Non-nanostructured	Nanostructured
D10 (nm)	979	133
D50 (nm)	1797	187
D90 (nm)	3359	276
D[3,2] (nm)	1631	183
D[4,3] (nm)	2006	197
Specific surface area ( $\text{m}^2/\text{g}$ )	3.679	32.828
Polydispersity index (PDI)	0.45	0.21

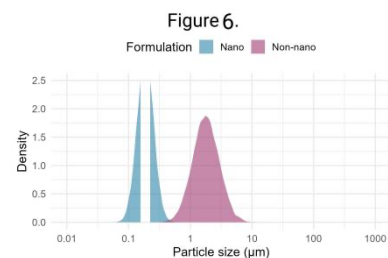


**Figure 6.** Particle size distribution overlay. Nano formulation shifts from micron-scale to nanoscale ( $D_{50} = 187 \text{ nm}$ ).

#### 3.1.2 Morphological Assessment

TEM imaging revealed distinct morphological differences (Figure 7). Non-nanostructured propolis appeared as irregular, heterogeneous aggregates; nanostructured propolis exhibited uniform spherical

nanoparticles with smooth surfaces and well-defined boundaries.

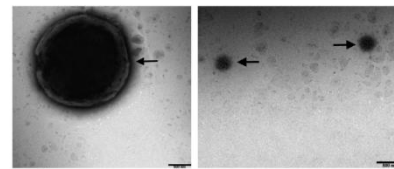
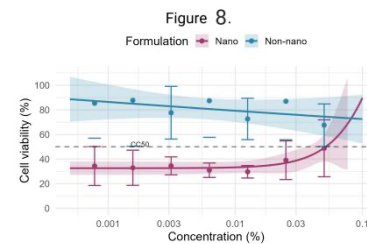


Figure 7. a. Non-nano propolis b. Nano propolis

**Figure 7.** TEM micrographs. (a) Non-nano propolis: irregular aggregates; (b) Nano propolis: uniform spherical nanoparticles. Scale bar = 500 nm.

### 3.2 Cytotoxicity Profile

Both formulations exhibited concentration-dependent cytotoxicity (Figure 8).  $CC_{50}$  values were 0.024% (95% CI: 0.021–0.027%) for non-nanostructured and 0.026% (95% CI: 0.023–0.029%) for nanostructured propolis ( $*p^* > 0.05$ ) (Table 2).



**Figure 8.** Concentration-dependent cytotoxicity.  $CC_{50} = 0.024\%$  (non-nano) and  $0.026\%$  (nano).

Table 2. Cytotoxicity parameters of propolis formulations in Vero cells.

Parameter	Non-nanostructured	Nanostructured
$CC_{50}$ (%)	0.024	0.026
95% confidence interval (%)	0.021–0.027	0.023–0.029

### 3.3 Antiviral Activity

#### 3.3.1 $IC_{50}$ Values and Selectivity Indices

Both formulations inhibited HSV-2 in a concentration-dependent manner (Figure 3).  $IC_{50}$  values were 0.003% for non-nanostructured and 0.004% for nanostructured propolis ( $*p^* > 0.05$ ). Selectivity indices were 60.0 and 86.7, representing a 44% improvement for the nanostructured formulation (Table 3, Figure 9).

Table 3. Antiviral activity parameters against HSV-2.

Parameter	Non-nanostructured	Nanostructured
$IC_{50}$ (%)	0.003	0.004
95% CI (%)	0.0025–0.0035	0.0034–0.0046
Selectivity index	60	86.7
Maximum inhibition at MNCC (%)	98.3	98.7

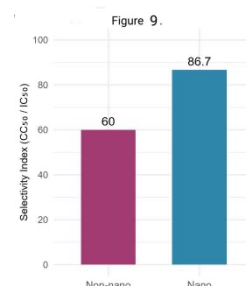


**Figure 9.** Selectivity indices.  $SI = 60.0$  (non-nano)

and 86.7 (nano), a 44% improvement.

### 3.3.2 Mechanism of Antiviral Action

Time-of-addition experiments demonstrated that propolis exerts its primary antiviral effect through direct virucidal activity (Figure 4). Virus pre-treatment resulted in near-complete plaque elimination ( $98.3 \pm 1.2\%$  and  $98.7 \pm 0.9\%$  suppression). Minimal activity was observed in cell pre-treatment (42–45% suppression) and post-adsorption (23–26% suppression). Complete plaque count data are summarized in Table 4.

Table 4. Summary of plaque reduction under all treatment conditions.

Treatment condition	Formulation	Plaques (mean $\pm$ SD)	Suppression (%)
Virus pre-treatment	Non-nano	1.0 $\pm$ 0.9	98.3 $\pm$ 1.2
	Nano	0.9 $\pm$ 0.9	98.7 $\pm$ 0.9
	ACV	24.4 $\pm$ 6.3	96.5 $\pm$ 1.8
Cell pre-treatment	Non-nano	29.3 $\pm$ 3.8	42.1 $\pm$ 5.6
	Nano	28.3 $\pm$ 3.2	44.8 $\pm$ 6.1
	ACV	32.4 $\pm$ 4.1	8.2 $\pm$ 3.4
Adsorption period	Non-nano	10.7 $\pm$ 3.7	58.7 $\pm$ 4.3
	Nano	11.8 $\pm$ 3.0	61.2 $\pm$ 5.0
	ACV	7.4 $\pm$ 1.5	94.1 $\pm$ 2.1
Post-adsorption	Non-nano	32.8 $\pm$ 2.3	23.4 $\pm$ 4.8
	Nano	30.5 $\pm$ 3.5	25.6 $\pm$ 5.2
	ACV	3.1 $\pm$ 1.8	97.3 $\pm$ 1.5
Virus control	–	39.2 $\pm$ 0.8	0

### 3.3.3 Viral Replication Kinetics

In untreated control cultures, viral titers increased exponentially from  $10^{3.50}$  TCID<sub>50</sub>/mL at 24 h to  $10^{6.167}$  TCID<sub>50</sub>/mL at 72 h. In nanostructured propolis-treated cultures, titers remained suppressed throughout (Figure 11). Log reductions were 0.25, 1.625, 2.784, and 2.400 at 24, 48, 72, and 96 h, respectively (Figure 10). Two-way ANOVA results are presented in Table 5.

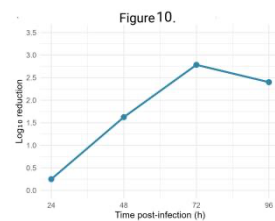


Figure 10. Log<sub>10</sub> reduction of HSV-2 titers over 96 h with nano propolis. Max reduction = 2.78 log<sub>10</sub> at 72 h.

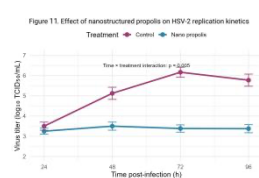


Figure 11. Two-way ANOVA interaction plot. Significant treatment effect ( $*p^* < 0.0001$ ) and time  $\times$  treatment interaction ( $*p^* = 0.005$ ).

Table 5. Two-way ANOVA results for viral replication kinetics.

Source	SS	df	MS	F	p-value
Time	2.45	3	0.817	10.2	0.002
Treatment	18.67	1	18.67	233.4	<0.0001
Time $\times$ Treatment	1.98	3	0.66	8.25	0.005
Residual	0.64	8	0.08		

## 4. Discussion

This study demonstrates that nanostructured Brazilian green propolis exerts potent virucidal activity against HSV-2 through direct interaction with extracellular virions, achieving sustained suppression of viral replication over 96 h. The nanostructured formulation improved the selectivity index by 44% while preserving full antiviral efficacy, addressing key physicochemical barriers to propolis clinical translation.

### 4.1 Physicochemical Enhancement

Nanostructured propolis (mean diameter 187 nm, PDI = 0.21) showed an 8.9-fold increase in specific surface area, which is expected to enhance dissolution rate and bioavailability.<sup>15</sup> TEM images confirmed uniform spherical morphology, consistent with DLS data.<sup>19</sup>

### 4.2 Cytotoxicity and Safety

The CC<sub>50</sub> values (0.024% and 0.026%) are consistent with literature on propolis cytotoxicity.<sup>14</sup> Nanostructuring did not increase toxicity, confirming the encapsulation materials are non-toxic at the concentrations used.

### 4.3 Antiviral Potency and Selectivity

IC<sub>50</sub> values (0.003% and 0.004%) closely match earlier reports on propolis anti-HSV activity,<sup>10,11</sup> indicating that nanostructuring does not compromise potency. The selectivity indices (60.0 and 86.7) far exceed those of other natural products. The 44% improvement in SI with nanostructuring suggests that encapsulation shields cells from cytotoxic constituents while allowing antiviral activity,<sup>15</sup> consistent with studies on nanoencapsulated natural products.

### 4.4 Mechanism of Action

Time-of-addition experiments definitively established that propolis exerts its primary antiviral effect through direct virucidal activity. Virus pre-treatment resulted in >98% plaque reduction, whereas post-adsorption treatment achieved only 23–26% suppression, confirming minimal intracellular activity.<sup>24</sup> For enveloped viruses, envelope disruption precludes attachment and fusion, rendering virions non-infectious. This explains propolis's retained activity against acyclovir-resistant strains. Recent work supports that propolis nanoparticles cause direct particle inactivation and downregulate HSV-2 replication genes.<sup>15</sup>

### 4.5 Sustained Suppression via “Extracellular

### Trap” Mechanism

Despite minimal intracellular activity, nanostructured propolis suppressed viral replication over 96 h (2.78 log<sub>10</sub> reduction at 72 h), revealing a secondary mechanism: inactivation of progeny virions as they are released from infected cells. This “extracellular trap” limits subsequent rounds of infection, accounting for sustained suppression in multistep growth curves.

### 4.6 Clinical Implications

The present in vitro findings are consistent with anecdotal clinical observations, where patients self-administering oral propolis reported reduced recurrence. These observations underscore the need for formal clinical trials. Based on these findings, we propose a clinical algorithm for propolis use in IVF patients (Supplementary Material S1).

### 4.7 Strengths and Limitations

Strengths include robust experimental design, comprehensive statistical analysis, definitive mechanistic elucidation, and methodological rigor. Limitations include the in vitro nature, use of a single virus strain, and absence of in vivo data. Future studies should evaluate activity against clinical isolates and acyclovir-resistant strains, and assess efficacy in animal models.

### 5. Conclusion

This study demonstrates that nanostructured Brazilian green propolis retains full antiviral potency against HSV-2 while achieving a 44% improved selectivity index. The definitive mechanistic evidence establishes direct virucidal activity targeting extracellular virions as the primary mechanism of action, with sustained replication suppression via an “extracellular trap” mechanism. These findings address the physicochemical limitations that have hindered propolis clinical translation and provide a mechanism-based translational framework positioning nanostructured propolis as a promising candidate for topical prophylactic use in ART patients.

### Acknowledgments

The authors thank the technical staff at the Department of Dermatovenereology and the Central Laboratory Facility for their assistance with cell culture and electron microscopy.

### Conflict of Interest

The authors declare no conflict of interest.

### Data Availability Statement

The data that support the findings of this study are available from the corresponding author upon reasonable request.

### References

1. Harfouche M, AlMukdad S, Alareeki A, et al. Estimated global and regional incidence and prevalence of herpes simplex virus infections and genital ulcer disease in 2020: mathematical modelling analyses. *Sex Transm Infect.* 2025;101(4):214-223.
2. Schiffer JT, Mayer BT, Fong Y, Swan DA, Wald A. Herpes simplex virus-2 transmission probability estimates based on quantity of viral shedding. *J R Soc Interface.* 2014;11(95):20140160.
3. Looker KJ, Elmes JA, Gottlieb SL, et al. Effect of HSV-2 infection on subsequent HIV acquisition: an updated systematic review and meta-analysis. *Lancet Infect Dis.* 2017;17(12):1303-1316.
4. Looker KJ, Welton NJ, Sabin KM, et al. Global and regional estimates of the contribution of herpes simplex virus type 2 infection to HIV incidence: a population attributable fraction analysis using published epidemiological data. *Lancet Infect Dis.* 2020;20(2):240-249. doi:10.1016/S1473-3099(19)30470-0
5. Schalkwijk HH, Snoeck R, Andrei G. Acyclovir resistance in herpes simplex viruses: Prevalence and therapeutic alternatives. *Biochem Pharmacol.* 2022;206:115322. doi:10.1016/j.bcp.2022.115322
6. Practice Committee of the American Society for Reproductive Medicine. Recommendations for reducing the risk of viral transmission during fertility treatment with the use of autologous gametes: a committee opinion. *Fertil Steril.* 2020;114(6):1158-1164. doi:10.1016/j.fertnstert.2020.09.133
7. Pasternak B, Hviid A. Use of acyclovir, valacyclovir, and famciclovir in the first trimester of pregnancy and the risk of birth defects. *JAMA.* 2010;304(8):859-866. doi:10.1001/jama.2010.1206
8. Sforcin JM. Biological properties and therapeutic applications of propolis. *Phytother Res.* 2016;30(6):894-905. doi:10.1002/ptr.5605
9. Park YK, Alencar SM, Aguiar CL. Botanical origin and chemical composition of Brazilian propolis. *J Agric Food Chem.* 2002;50(9):2502-2506. doi:10.1021/jf011432b
10. Amoros M, Lurton E, Boustie J, et al. Comparison of the anti-herpes simplex virus activities of propolis and 3-methyl-but-2-enyl caffeate. *J Nat Prod.* 1994;57(5):644-647. doi:10.1021/np50107a013

11. Schnitzler P, Neuner A, Nolkemper S, et al. Antiviral activity and mode of action of propolis extracts and selected compounds. *Phytother Res.* 2010;24(S1):S20-S28. doi:10.1002/ptr.2868
12. Kujumgiev A, Tsvetkova I, Serkedjieva Y, Bankova V, Christov R, Popov S. Antibacterial, antifungal and antiviral activity of propolis of different geographic origin. *J Ethnopharmacol.* 1999;64(3):235-240. doi:10.1016/S0378-8741(98)00131-7
13. Burdock GA. Review of the biological properties and toxicity of bee propolis (propolis). *Food Chem Toxicol.* 1998;36(4):347-363. doi:10.1016/S0278-6915(97)00145-2
14. Lawrence MJ, Rees GD. Microemulsion-based media as novel drug delivery systems. *Adv Drug Deliv Rev.* 2000;45(1):89-121. doi:10.1016/S0169-409X(00)00103-4
15. Sangboonruang S, Semakul N, Sookkree S, et al. Activity of propolis nanoparticles against HSV-2: promising approach to inhibiting infection and replication. *Molecules.* 2022;27(8):2560. doi:10.3390/molecules27082560
16. Hierholzer JC, Killington RA. Virus isolation and quantitation. In: *Virology Methods Manual.* Academic Press; 1996:25-46.
17. Date AA, Nagarsenker MS. Design and evaluation of microemulsions for improved parenteral delivery of propofol. *AAPS PharmSciTech.* 2008;9(1):138-145. doi:10.1208/s12249-007-9023-7
18. Pouton CW. Lipid formulations for oral administration of drugs: non-emulsifying, self-emulsifying and 'self-microemulsifying' drug delivery systems. *Eur J Pharm Sci.* 2000;11 Suppl 2:S93-S98. doi:10.1016/S0928-0987(00)00167-6
19. Danaei M, Dehghankhold M, Ataei S, et al. Impact of particle size and polydispersity index on the clinical applications of lipidic nanocarrier systems. *Pharmaceutics.* 2018;10(2):57. doi:10.3390/pharmaceutics10020057
20. Kuntsche J, Horst JC, Bunjes H. Cryogenic transmission electron microscopy (cryo-TEM) for studying the morphology of colloidal drug delivery systems. *Int J Pharm.* 2011;417(1-2):120-137. doi:10.1016/j.ijpharm.2011.02.001
21. Mosmann T. Rapid colorimetric assay for cellular growth and survival: application to proliferation and cytotoxicity assays. *J Immunol Methods.* 1983;65(1-2):55-63. doi:10.1016/0022-1759(83)90303-4
22. Ritz C, Baty F, Streibig JC, Gerhard D. Dose-response analysis using R. *PLoS One.* 2015;10(12):e0146021. doi:10.1371/journal.pone.0146021
23. Pauwels R, Balzarini J, Baba M, et al. Rapid and automated tetrazolium-based colorimetric assay for the detection of anti-HIV compounds. *J Virol Methods.* 1988;20(4):309-321. doi:10.1016/0166-0934(88)90134-6
24. Schnitzler P, Koch C, Reichling J. Susceptibility of drug-resistant clinical herpes simplex virus type 1 strains to essential oils of ginger, thyme, hyssop, and sandalwood. *Antimicrob Agents Chemother.* 2007;51(5):1859-1862. doi:10.1128/AAC.00426-06

**Supplementary Materials**

**Supplementary Figure S1.** Proposed clinical management algorithm for HSV-2 infection during IVF treatment.